Large Enhancement of Magnetoresistance in $Tl_2Mn_2O_7$: Pyrochlore Versus Perovskite

A. P. Ramirez and M. A. Subramanian

The synthesis of and magneto-transport in the "colossal magnetoresistance" (CMR) pyrochlore-structure compounds $Tl_{2-x}Sc_xMn_2O_7$ for $0 \leq x \leq 0.5$ are reported. The maximum resistivity (ρ) increases by 10^5 while the Curie temperature (T_c) decreases by only 25% between $x = 0$ and 0.4. For $x = 0.2$ to 0.3, the magnetoresistance at both high field (6 tesla) and low field (<0.05 tesla) are significantly enhanced over the undoped ($x = 0$) compound. Structural analysis indicates that all of the manganese ions are near the +4 oxidation state. The behavior of ρ and T_c suggests that scandium substitution affects mainly electronic conduction on the thallium-oxygen sublattice while leaving the magnetism essentially unchanged. These results demonstrate a distinct way of manipulating magneto-transport properties in CMR materials.

The manganite perovskites—like $T_{1-x}D_xMnO_3$, where T is a trivalent element such as La or Bi and D is a divalent element such as Ca, Sr, or Pb—exhibit large magnetoresistance (known as CMR) associated with a transition from a low-temperature metallic-ferromagnetic to a high-temperature semiconducting-paramagnetic phase. This effect has been widely discussed in the context of magnetic sensing. The underlying physical mechanism associated with this transition is attributed to double exchange, a microscopic process in which carrier hopping is enhanced when neighboring Mn ions have mutually aligned spins (*1*). The occurrence of a metallic-ferromagnetic state for x between 0.2 and 0.5 is now thought to be related to the band-narrowing that arises from large electron-phonon coupling (*2*, *3*). The mechanism developed for CMR in the perovskites cannot easily be applied to the pyrochlore compound $Tl_2Mn_2O_7$, however. Here, the high-temperature state is metallic (*4*), there is no large mixed valency among Mn ions (*5*), and the Tl-O(I) sublattice is thought to contribute to states at the Fermi level (*5*).

One possible explanation for the CMR effect in $Tl_2Mn_2O_7$ is strong scattering of conduction electrons by spin fluctuations (SFs) associated with ferromagnetic (FM) ordering on the Mn-O sublattice (*6*). Scattering by SFs is usually a small effect, and in transition metals, for example, resistance changes of only a few percent occur near the FM ordering temperature T_c (*7*). The starting point for a SF scenario is the presence of two distinct electronic subsystems, itinerant (weakly magnetic) and localized (strongly magnetic). In $Tl_2Mn_2O_7$ pyrochlore, there is evidence for two such subsystems: (i) The itinerant system contains a significant admixture of Tl 6*s* electrons, as inferred from band structure calculations (*8*) and the systematics of transport among pyrochlores having different M^{3+} ions at the Tl site (*5*), and (ii) the local-moment system is comprised of Mn 3*d* electrons, as inferred from the large FM moments observed in other Mn-O pyrochlores and the similarity of the Mn-O-Mn bonding among these compounds. Pyrochlores differ from transition metals and the Eu-chalcogenides, which also display CMR, in that the itinerant and localized subsystems originate from distinct lattice sites. Besides the two-sublattice feature, the pyrochlores differ from typical SF systems in the carrier density n. In $Tl_2Mn_2O_7$, $n = 1 \times 10^{-3}$ to 5×10^{-3} electrons per formula unit, whereas one would expect $n \approx 1$ for a metal (*4*).

Because magnetism and transport in the pyrochlores originate from distinct atom sites, it is possible to independently tune the materials parameters relevant in a SF model. Here we study the effect of substituting Sc for Tl in $Tl_{2-x}Sc_xMn_2O_7$. Scandium is trivalent like Tl, but it has a smaller ionic radius and no accessible empty 6*s* level. We found that Sc substitution has a dramatic effect on electronic transport. Over a wide temperature range (150 to 200 K) in the paramagnetic phase, the resistivity ρ increases by five orders of magnitude as x goes from 0 to 0.4. In addition, the magnetoresistance MR(H), defined as $[R(0) - R(H)]/R(H)$, at magnetic fields $H = 6$ T increases by a factor of 60 between $x = 0$ and 0.2, and at low fields, MR(0.05) is also significantly enhanced. Similar enhancements in MR(H) were found in the Mn-O perovskites but are always accompanied by strong suppression (~100%) of the FM Curie temperature T_c (*9*). In the Sc-substituted $Tl_2Mn_2O_7$ pyrochlores, however, the suppression of T_c accompanying the rise in MR(H) is much smaller (~15%). This result demonstrates the possibility, in principle, to induce large increases in MR while leaving T_c effectively unchanged. This property, a desirable feature for applications, is characteristic of the two–electronic-sublattice pyrochlore compound and motivates further materials searches.

Appropriate quantities of high-purity Tl_2O_3, Sc_2O_3, and MnO_2 were mixed together in an agate mortar and sealed in a gold capsule. The capsule was heated to 900°C for 30 min at 5.8 GPa in a tetrahedral anvil press and then rapidly cooled to room temperature before the pressure was released. All of the peaks in powder x-ray diffraction (XRD) data for $Tl_{2-x}Sc_xMn_2O_7$ samples ($x = 0.05$, 0.1, 0.2, 0.3, and 0.4) could be indexed with a cubic unit cell (space group $Fd\bar{3}m$), and no additional reflections resulting from impurities were observed. The refined lattice parameters showed a systematic decrease with Sc substitution, consistent with the significantly smaller octahedral ionic radius for Sc^{3+} compared with that for Tl^{3+}. Electron microprobe analysis of the samples showed that the compounds are stoichiometric and agreed well with the starting compositions (±1%). However, for samples with $x \geq 0.5$, the XRD patterns showed peak splitting, especially at higher 2θ values, indicating that the samples are biphasic. Microscopic examination of $Tl_{1.8}Sc_{0.2}Mn_2O_7$ revealed several small single crystals, which were recovered and used for single-crystal XRD refinement, collected at 296 K on an Enraf-Nonius CAD-4 diffractometer [details are given in (*5*)]. The dc magnetization *M* was measured with a commercial SQUID (superconducting quantum interference device) magnetometer. Resistivity measurements were made with the use of a dc method and a four-probe in-line configuration. Thermopower was measured in a thermocouple configuration referenced to constantan.

The $A_2M_2O_7$ pyrochlore structure can be viewed as two interpenetrating networks: one with corner-shared MO_6 octahedra giving rise to a network composition $MnO(II)_3$, and the other forming intersecting A-O(I) chains with a formula $A_2O(I)$ (Fig. 1). In the case of $A_2Mn_2O_7$ pyrochlores, the compounds are electrically insulating when A is a rare earth element, Y, or Sc, whereas when A is Tl, the compound is highly conducting and shows long-range FM order. As mentioned previously, the high conductivity in $Tl_2M_2O_7$ and its strong interdependence on the magnetic moment is apparently due to the mixing of Tl 6*s* bands with Mn t_{2g} bands at the Fermi level, a view supported by recent band structure calculations (*8*). Thus, Sc substitution should effect CMR both through modulation of the lattice constant as well by introduction of disorder on the Tl-O(1) sublattice.

A. P. Ramirez, Bell Laboratories, Lucent Technologies, 600 Mountain Avenue, Murray Hill, NJ 07974-0636, USA.
M. A. Subramanian, DuPont Central Research and Development, Experimental Station, Wilmington, DE 19880-0328, USA.

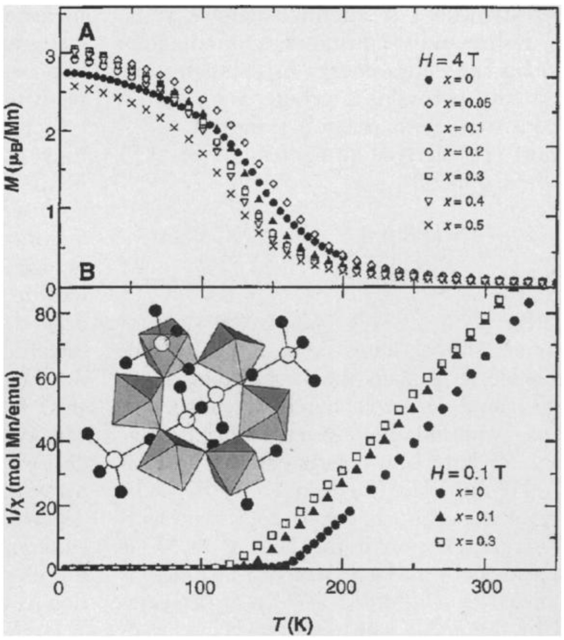

Fig. 1. (**A**) Magnetization of $Tl_{2-x}Sc_xMn_2O_7$ versus temperature at an applied field of 4 T for different values of *x*. (**B**) Inverse susceptibility versus temperature for compounds of different values of *x* (in moles of Mn per electromagnetic unit). (**Inset**) Schematic view of the structure of $Tl_{2-x}Sc_xMn_2O_7$, emphasizing the interpenetrating networks of $MnO(II)_6$ octahedra and the $(Tl,Sc)_2O(I)$ unit. Small filled circles represent (Tl,Sc) atoms, and the large open circles represent O(I) oxygens.

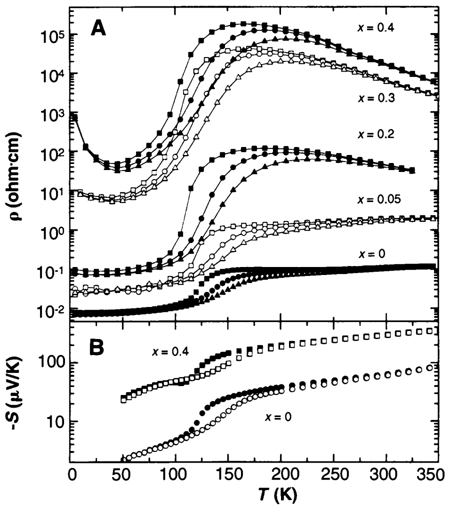

Fig. 2. (**A**) Resistivity versus temperature of $Tl_{2-x}Sc_xMn_2O_7$ for various values of *x*. The upper, middle, and lower curves for each *x* correspond to applied fields of *H* = 0, 3, and 6 T, respectively. (**B**) Thermopower versus temperature for *x* = 0 and 0.4 at *H* = 0 T (filled) and 6 T (open).

The structural refinement of $Tl_{1.8}Sc_{0.2}Mn_2O_7$ (Table 1) shows that the compound is stoichiometric with respect to Tl (Sc), Mn, and O, agreeing with chemical analysis. The observed Mn-O distance of 1.90 Å for $Tl_{1.8}Sc_{0.2}Mn_2O_7$ is essentially the same as that for $Tl_2Mn_2O_7$ (Table 1) and is near the expected value based on the sum of the ionic radii of Mn^{4+} and O^{2-} (*10*). The similar distances again rule out the possibility for Mn^{3+}-Mn^{4+} double exchange in Sc-substituted phases. Although the Mn-O(II) distance changes negligibly, the Tl(Sc)-O(I) distances do show notable changes upon Sc substitution for Tl in $Tl_2Mn_2O_7$. In the pyrochlore structure, the A atoms are situated in the center of puckered hexagonal rings formed by six O(II) atoms, with two additional O(I) atoms located below and above the ring. The A-O(I) distance is always slightly shorter than the A-O(II) distance. The observed decrease in the Tl(Sc)-O(II) and Tl(Sc)-O(I) bond distances in $Tl_{1.8}Sc_{0.2}$ Mn_2O_7 indicates that the Sc atoms substitute in the Tl sites exclusively. However, the Tl-O(II) bond length decreases nearly twice as much as does the Tl(Sc)-O(I) bond length. This difference is primarily due to the higher oxygen affinity of Sc^{3+}. With an electronic configuration of $3d^0$, Sc^{3+} prefers a more regular environment [by drawing the six O(II) atoms closer to it], whereas Tl^{3+}, which has a readily polarizable electronic configuration of $5d^{10}6s^0$, prefers a more distorted environment. Thus, the main effect of the shrinking of the lattice with Sc substitution is the reduction of the Tl-O(II)(-Mn) distance, which one then expects to increase the interaction (covalent mixing) between the two sublattices. However, at the same time, the inclusion of Sc on the Tl-O(I) sublattice localizes the conduction electrons, because of the inaccessibility of the Sc *s* states, which makes the Sc atoms strong scattering sites. These competing tendencies affect the magnetism and transport.

The *M*(*T*) data at 4 T (Fig. 1A) show that for *x* = 0, the low-temperature saturation value ($M_s = 2.8\mu_B$, where μ_B is the Bohr magneton) is close to that expected for Mn^{4+} ($M_s = 3\mu_B$), as found earlier (*4*, *5*). As *x* increases, M_s first increases toward $3.05\mu_B$ for *x* = 0.3 and then gradually decreases. This small increase in M_s might be related to the increased covalent mixing mentioned above. Most important, however, is the relative insensitivity of M_s to *x*: Indeed, $M_s = 2.75\mu_B$ for the end member $Sc_2Mn_2O_7$, which is an insulator (*11*). In the paramagnetic region, the inverse susceptibility $1/\chi$ at 0.1 T (Fig. 1B) shows a systematic decrease of the Weiss constant θ_W [defined by $1/\chi = C/(T - \theta_W)$, where C is a Curie constant] with increasing *x*. This decrease is consistent with the temperature of sharpest magnetization change, inferred from high-field data. It is interesting to compare the change in T_c (Table 2), the temperature of greatest curvature in the low-field $1/\chi(T)$ data, to a comparable lattice-constant reduction in the perovskite system. Hwang *et al.* (*12*) found that *a* increases from 3.855 to 3.868 Å between $Pr_{0.7}Ca_{0.3}MnO_3$ and $La_{0.525}Pr_{0.175}Ca_{0.3}$ MnO_3. This 0.3% increase in *a* is accompanied by a 55% reduction in T_c, from 250 to 110 K. A similar fractional decrease in *a* was found for $Tl_{2-x}Sc_xMn_2O_7$ between *x* = 0 and 0.3, but T_c decreased by only 22%. This result suggests a smaller magnetorestrictive coupling in the pyrochlores than in the perovskites.

In contrast to the magnetization data, which show modest changes as a function of *x*, ρ(*T*) (Fig. 2) increases by several orders of magnitude as *x* is increased from 0 to 0.4. These data are in contrast to those found for

Table 1. Structure data (single-crystal x-ray diffraction) for $Tl_2Mn_2O_7$ and $Tl_{1.8}Sc_{0.2}Mn_2O_7$ pyrochlores. Atomic positions: Tl (Sc) 16*d*(1/2, 1/2, 1/2); Mn 16*c*(0, 0, 0); O(I) 8*b*(3/8, 3/8, 3/8); and O(II) 48*f* (*x*, 1/8, 1/8). Values of the ionic radii for eightfold coordinated $(Tl,Sc)^{3+}$ are from (*10*). The data for $Tl_2Mn_2O_7$ are taken from (*5*). Numbers in parentheses are the error in the last digit.

Parameter	$Tl_2Mn_2O_7$	$Tl_{1.81(1)}Sc_{0.19(1)}Mn_2O_7$*
Lattice parameter (Å)	9.892(1)	9.869(1)
Mn-O(II) (×6) (Å)	1.901(1)	1.900(1)
Tl (Sc)-O(II) (×6) (Å)	2.458(1)	2.447(1)
Tl (Sc)-O(I) (×2) (Å)	2.142(1)	2.137(1)
Mn-O(II)-Mn angle (degrees)	133.8(1)	133.4(1)
x in O(II) 48*f* (*x*, 1/8, 1/8)	0.3254(8)	0.3260(5)
R factor (%)†	1.6	2.4
Average ionic radius of $(Tl,Sc)^{3+}$ (Å)	0.98	0.969

*Composition is derived from the microprobe data and agrees well with the occupancy factors refined from single-crystal data. †All atoms were refined anisotropically.

the case of In substitution in $Tl_{2-x}In_xMn_2O_7$ (*13*), where ρ(300 K) for $x = 0.25$ is only a factor of 3 greater than that for $x = 0$. A similar doping level of Sc leads to an increase of almost three orders of magnitude. Because the lattice-parameter change found with In substitution is comparable to that seen for Sc substitution, the large difference in ρ must be related to the different electronic configurations of the two dopant species. The 5*s* levels of In are expected to have greater overlap with the Tl 6*s* band than either the *d* or *s* levels in Sc and therefore would be expected to produce a smaller change in transport. The large increase in $\rho(T)$ is unlikely to be related to oxygen off-stoichiometry for several reasons: (i) the absence of a large effect for In substitution, despite its chemical similarity to Sc; (ii) our inability to make $Ln_2Mn_2O_7$ (Ln = Dy-Lu, Y, Sc) conduct by reduction; and (iii) the systematic changes in ρ with Sc concentration and its correlation with lattice constant.

To further understand the role of Sc in producing large changes in $\rho(T)$, we performed Hall effect ($x = 0.3$) and thermopower S (for $x = 0$ and 0.4) measurements. For $x = 0.3$ and $T = 50$ K, the absence of a measurable Hall voltage above the noise implies a lower bound of $n \approx 5 \times 10^{-4}$ carriers per formula unit, 10 to 50% of that found for $x = 0$ (*4*). Although large increases in ρ can occur for modest decreases in n in extrinsic semiconductors (*14*), the present increase by a factor of 10^5 in ρ accompanying this lower bound on n suggests there is also a change in scattering time. Because of the small spatial extent of the Sc 4*s* orbital, it is reasonable to assume that Sc introduces a strong-scattering 6*s* vacancy into the Tl-O(I) network. The introduction of such vacancies is contrary to what occurs in the perovskites, where modification of the transport is achieved by charge transfer between the electronically inactive A site and the Mn-O sublattice. The qualitative difference between the "doping" dependencies of both systems is also manifested in $S(T)$. For $x = 0$, $S(T > T_c)$ behaves as expected for a metal with a low carrier density, where the thermal energy k_BT (k_B is Boltzmann's constant) approximately equals the Fermi energy E_F, behavior unlike the perovskites, where $S(T) \propto 1/T$ [consistent with polaron transport (*15*)]. Mott (*16*) derived an expression for $S(T)$ in a FM metal

$$S = \frac{\pi^2 k^2 T}{3|e|}\left(\frac{3}{2E_F} - \frac{N'_\uparrow + N'_\downarrow}{N}\right) \qquad (1)$$

where $N'_{\uparrow,\downarrow} = dN_{\uparrow,\downarrow}/dE$ is the slope of the density of states N at E_F. It is thus possible to explain the large reduction in $S(T)$ at T_c by invoking large changes in $N'_{\uparrow,\downarrow}$ with FM ordering, a plausible assumption for large spin polarization and a small E_F. For finite H, $S(T)$ decreases in the vicinity of T_c. This change is consistent with Mott's expression if the change in N' is spread out over a larger temperature range, as implied by a $|dM/dT|$ at T_c that decreases with the field. The differing behavior of $S(T)$ exhibited by perovskite and pyrochlore ($x = 0$) in the paramagnetic state is not surprising given that they exhibit semiconducting-type and metallic resistivity, respectively. However, for the $x = 0.4$ pyrochlore (Fig. 2B), even though $d\rho/dT < 0$ in the paramagnetic regime, $dS/dT > 0$, unlike the polaron behavior describing the perovskites (*15*). (For either intrinsic or hopping-type semiconductors, one expects $S \sim \ln \rho$, and thus, the factor of 5 increase between $x = 0$ and 0.4 mirrors the change by several orders of magnitude in ρ.) Therefore, the gross features of the metal-to-insulator transition induced by an increase in x are qualitatively different from those seen in the perovskite CMR materials.

If x is increased from 0 to 0.2 in $Tl_{2-x}Sc_xMn_2O_7$, MR(6 T) (Fig. 3) changes from 0.9 to 58. Such a large enhancement of MR(H) in the perovskites has been observed by several methods. For example, Jin *et al.* (*9*) reported enhancements of 10^2 in $La_{1-x}Ca_xMnO_3$ films; Tokura *et al.* (*17*) found hysteretic decreases in $R(H)$ of several orders of magnitude associated with a structural transition in $(Nd,Sm)_{0.5}Sr_{0.5}MnO_3$; and Hwang *et al.* (*12*) studied the systematic increase of MR with decreasing lanthanide radius in $La_{0.7-y}Pr_yCa_{0.3}MnO_3$. The correlation between MR(H) and T_c has been directly addressed by Khazeni *et al.* (*18*), who compiled results from various studies (Fig. 3, inset). Despite the generally lower values of MR(6 T), T_c for the pyrochlores is much less sensitive to relative changes in MR than is T_c for the perovskites. This behavior strongly suggests that, to a first approximation, the localized electron Mn-O sublattice acts independently of the itinerant-electron Tl-O sublattice.

Finally, we present the low-field MR(H) (Fig. 4A). At low temperatures ($T = 20$ and 60 K), there is an abrupt initial decrease in $R(H)/R(0)$ similar to that seen in perovskite materials and attributed to spin-dependent transport across grain boundaries (intergrain contribution), consistent with the sharp initial increase of the magnetization M (Fig. 4B) (*19*, *20*). Above $H = 0.05$ T for $T = 20$ and 60 K, the magnitude of dR/dH decreases dramatically (intragrain contribution). There is a large temperature dependence of the intragrain dR/dH for $H < 0.1$ T, especially as $T \rightarrow T_c$ from below. This dependence leads to an initial slope of the intragrain contribution at $T = 110$ K that is comparable to that of the intergrain contribution at much lower T. For the pyrochlore $Tl_{2-x}Sc_xMn_2O_7$ at $x = 0$, the initial slope magnitude (obtained from a linear fit for $0 < H < 0.05$ T) is greater than that for the perovskite $La_{0.7}Ca_{0.3}MnO_3$ (Fig. 4C). This difference is perhaps not surprising, given the large difference in the values of T_c between the two compounds. What is notable, however, is the large difference in slope magnitude between the $x = 0$ and $x = 0.3$ pyrochlores:

Table 2. Variation of the structural and physical parameters as a function of Sc concentration in $Tl_{2-x}Sc_xMn_2O_7$.

x	Lattice parameter (Å)	T_c (K)	M_s (μ_B)	ρ(300 K) (ohm·cm)
0	9.892	158	2.75	1.1×10^{-1}
0.05	9.888	161	3.03	1.9×10^0
0.1	9.881	135	2.98	7.4×10^1
0.2	9.868	125	2.93	4.5×10^1
0.3	9.855	123	3.05	6.6×10^3
0.4	9.845	120	3.03	1.7×10^4
0.5*		117	2.56	–

*Material is biphasic at this concentration.

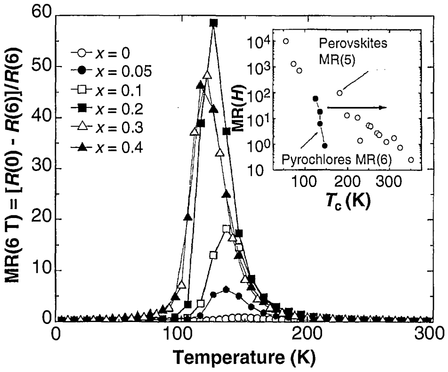

Fig. 3. Magnetoresistance versus temperature of $Tl_{2-x}Sc_xMn_2O_7$ pyrochlores for various values of x. (**Inset**) The maximum magnetoresistance versus ordering temperature for the pyrochlores (open symbols) and the manganite perovskites (closed symbols) [data from (*18*)]. The arrow symbolizes the expected shift of the pyrochlore data if the exchange interaction among Mn-site ions could be increased.

While T_c decreases by only 20%, $|dR/dH|$ increases by a factor of 4.

The above results illustrate the distinct magneto-transport in the Sc-substituted pyrochlores. In particular, there is no evidence in the systematics of $\rho(T)$ and $S(T)$ of a polaron mechanism like that shown for the perovskites (*15*). Instead, we propose that the pyrochlores are closer to the Cr spinels (*21*), where large (10^4) decreases in $\rho(T)$ (such as in $CdCr_2Se_4$) have been modeled in terms of a FM-ordering–induced modification of a mobility edge (*22*). The Cr spinels bear more than a superficial resemblance to the pyrochlores: Both are low-*n* systems, both have electronically active A sites, and both exhibit a low-*T* upturn in $\rho(T)$. It would be of interest to extend the theory developed for the Cr spinels to the present case, especially for the purpose of understanding the large MR and its interdependence on T_c.

We have shown that MR near T_c is greatly enhanced in the pyrochlores $Tl_2Mn_2O_7$ with substitution of Sc for Tl, nearly independently of the precise value of T_c. This demonstrates a different paradigm for manipulating MR for magnetic-sensing applications. One of the drawbacks of the perovskites is that the bulk MR can be increased by chemical modification only at the expense of lowering T_c. At present, MR in the pyrochlores only occurs below 200 K, but it may be possible to achieve large MR at room temperature with the use of magnetic ions with larger exchange energies and hence larger values of T_c. Such systems might then be amenable to having their MR increased by chemical substitution as in $Tl_{2-x}Sc_xMn_2O_7$.

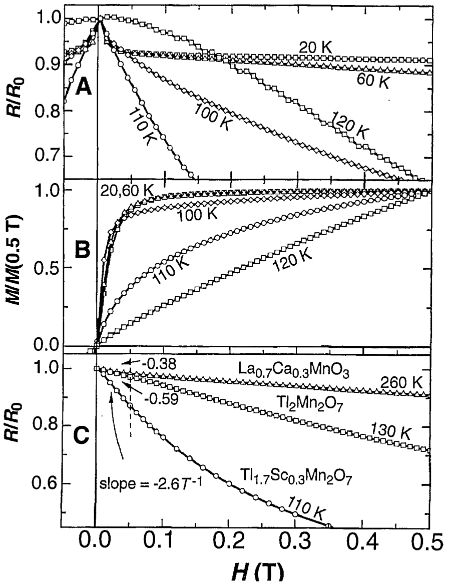

Fig. 4. (**A**) Field dependence of the resistance, normalized to the zero-field value for $Tl_{1.7}Sc_{0.3}Mn_2O_7$ for several temperatures near T_c. Data at small negative field values show an absence of hysteresis. (**B**) Magnetization versus field, normalized to the value at 0.5 T, for various temperatures. (**C**) Normalized resistance versus field for $La_{0.7}Ca_{0.3}MnO_3$, $Tl_2Mn_2O_7$, and $Tl_{1.7}Sc_{0.3}Mn_2O_7$ at the temperature where the intragrain contribution is maximized for each sample.

REFERENCES

1. C. Zener, *Phys. Rev.* **82**, 403 (1951); P.-G. de Gennes, *ibid.* **118**, 141 (1960).
2. A. J. Millis, B. I. Shraiman, R. Mueller, *Phys. Rev. Lett.* **77**, 175 (1996).
3. H. Röder, J. Zhang, A. R. Bishop, *ibid.* **76**, 1356 (1996).
4. Y. Shimikawa, Y. Kubo, T. Manako, *Nature* **379**, 53 (1996).
5. M. A. Subramanian *et al.*, *Science* **273**, 81 (1996).
6. M. E. Fisher and J. S. Langer, *Phys. Rev. Lett.* **20**, 665 (1968).
7. R. M. White and T. H. Geballe, *Long Range Order in Solids* (Academic Press, New York, 1979).
8. D.-K. Seo, M.-H. Whangbo, M. A. Subramanian, *Solid State Commun.* **101**, 417 (1997); D. J. Singh, *Phys. Rev. B* **55**, 313 (1997); S. F. Matar, M. A. Subramanian, J. Etourneau, *J. Mater. Chem.*, in press.
9. S. Jin *et al.*, *Science* **264**, 413 (1994).
10. R. D. Shannon, *Acta Crystallogr.* **32**, 751 (1976).
11. J. E. Greedan, N. P. Raju, M. A. Subramanian, *Solid State Commun.* **99**, 399 (1996).
12. H. Hwang, S-W. Cheong, P. G. Radaelli, M. Marezio, B. Batlogg, *Phys. Rev. Lett.* **75**, 914 (1995).
13. S-W. Cheong, H. Y. Hwang, B. Batlogg, L. W. Rupp Jr., *Solid State Commun.* **98**, 163 (1996).
14. H. J. Fritzsche, *J. Phys. Chem. Solids* **6**, 69 (1958).
15. M. Jaime *et al.*, *Appl. Phys. Lett.* **68**, 1576 (1996).
16. N. F. Mott, *Proc. R. Soc. London Ser. A* **156**, 368 (1936).
17. Y. Tokura, H. Kuwahara, Y. Moritomo, Y. Tomioka, A. Asamitsu, *Phys. Rev. Lett.* **76**, 3184 (1996).
18. K. Khazeni *et al.*, *ibid.*, p. 295.
19. P. Schiffer, A. P. Ramirez, W. Bao, S.-W. Cheong, *ibid.* **75**, 3336 (1995); H. Y. Hwang, S.-W. Cheong, N. P. Ong, B. Batlogg, *ibid.* **77**, 2041 (1996); A. Gupta *et al.*, *Phys. Rev. B* **54**, R15629 (1996).
20. The tunneling contribution in pure $Tl_2Mn_2O_7$ has been studied by H. Hwang and S.-W. Cheong (private communication).
21. A. P. Ramirez, R. J. Cava, J. Krajewski, *Nature* **386**, 156 (1997).
22. E. M. Kogan and M. I. Auslender, *Phys. Status Solidi* **147**, 613 (1988).

23. We would like to acknowledge M. L. Plummer and T. G. Calvarese (both at DuPont) for the high-pressure synthesis experiments and W. J. Marshall (DuPont) for the single-crystal diffractometry data. We acknowledge G. Kotliar, P. Littlewood, P. Majumdar, A. Millis, A. W. Sleight, and H. Y. Hwang for useful discussions and thank A. W. Sleight and P. Majumdar for a critical reading of the manuscript.

5 February 1997; accepted 9 June 1997

Spontaneous Oscillation and Self-Pumped Phase Conjugation in a Photorefractive Polymer Optical Amplifier

A. Grunnet-Jepsen, C. L. Thompson, W. E. Moerner

Optical processing with photorefractive polymers depends on achieving high optical gain, which depends exponentially on the product of the interaction length and the gain coefficient. By use of several polymer layers to increase the overall interaction length and a new high-performance photorefractive polymer composite, the overall optical one-pass gain becomes as large as a factor of 5. For a two-layer sample placed in an optical cavity made with two concave mirrors, spontaneous oscillation due to two-beam coupling gain was observed. Because only one pumping beam is required, this configuration also acts as a self-pumped phase-conjugating mirror with a reflectivity of 13 percent for an applied electric field of 75 volts per micrometer, marking a milestone for this growing class of optoelectronic materials.

The photorefractive (PR) effect refers to optically induced redistribution of charge in an electro-optic material to produce a spatial modulation of the refractive index, or a hologram (*1*). Inorganic crystals showing the PR effect have been known for more than 30 years, and a variety of applications for optical storage and processing have been suggested (*2*). An intriguing new materials class, the PR polymers, are attractive for applications owing to their ease of processing and low cost and, since their inception in 1991 (*3*), many new materials are showing the potential for high performance (*4*–*6*). The design of a PR polymer requires combining photoconductivity and optical nonlinearity in the same material, and to achieve this, an interdisciplinary combination of synthetic organic chemistry, nonlinear optics, and physical characterization is required (*7*). To illustrate the design strategy, the components of the material used in this study are shown in Fig. 1: (i) Charge (hole) transport is provided by poly(*n*-vinyl carbazole) (PVK); (ii) photoinduced charge generation at red wavelengths is provided by the fullerene C_{60} (*8*); (iii) the electro-optic response is provided by the nonlinear optical chromophore PDCST, which is oriented by an applied electric field; and (iv) lowering of the glass transition temperature

---

Department of Chemistry and Biochemistry, University of California, San Diego, CA 92093–0340, USA.